Design and Performance of the EO-1 Advanced Land Imager

Donald E. Lencioni *, Constantine J. Digenis
William E. Bicknell, David R. Hearn, Jeffrey A. Mendenhall
Massachusetts Institute of Technology - Lincoln Laboratory
244 Wood Street, Lexington, MA 02420-9185

ABSTRACT

An Advanced Land Imager (ALI) will be flown on the first Earth Observing mission (EO-1) under NASA's New Millennium Program (NMP). The ALI contains a number of key NMP technologies. These include a 15° wide field-of-view, push-broom instrument architecture with a 12.5 cm aperture diameter, compact multispectral detector arrays, non-cryogenic HgCdTe for the short wave infrared bands, silicon carbide optics, and a multi-level solar calibration technique. The focal plane contains multispectral and panchromatic (MS/Pan) detector arrays with a total of 10 spectral bands spanning the 0.4 to 2.5 μm wavelength region. Seven of these correspond to the heritage Landsat bands. The instantaneous fields of view of the detectors are 14.2 μrad for the Pan band and 42.6 μrad for the MS bands. The partially populated focal plane provides a 3° cross-track coverage corresponding to 37 km on the ground. The focal plane temperature is maintained at 220 K by means of a passive radiator. The instrument environmental and performance testing has been completed. Preliminary data analysis indicates excellent performance. This paper presents an overview of the instrument design, the calibration strategy, and results of the pre-flight performance measurements. It also discusses the potential impact of ALI technologies to future Landsat-like instruments.

Keywords: EO-1, multispectral, ALI, Landsat, calibration

1. INTRODUCTION

The first Earth-Observing satellite (EO-1) in the New Millennium Program (NMP) of the National Aeronautics and Space Administration (NASA) will carry an Advanced Land Imager (ALI) with multispectral imaging capability. The NMP missions are structured to accelerate the flight validation of advanced and enabling technologies. These technology validations are accomplished in the context of science measurement objectives. The focus of EO-1 is the validation of those technologies relevant to future Landsat missions. The ALI has been designed to produce images directly comparable to those from the Enhanced Thematic Mapper Plus (ETM+) of Landsat 7. The ALI will also establish data continuity with previous Landsats and demonstrate advanced capability and innovative approaches to future land imaging. The EO-1 satellite will fly "in formation" with the Landsat 7 satellite in a sun-synchronous, 705 km orbit with a 10:01 AM descending node. That is, it will be in an orbit that covers the same ground track approximately one minute later than the Landsat 7 satellite. Images of the same ground areas obtained by the two instruments at nearly the same time will be available for direct comparison by members of the science community. Accordingly, the basic field of view, angular resolution, and spectral bands are matched to those of the ETM+. Furthermore, the evaluation of on-orbit performance of the ALI technologies will provide timely information for the development of the next generation Landsat. The EO-1 satellite is co-manifested with Argentina's SAC-C (Scientific Applications Satellite) and is scheduled for launch from the Western Test Range on a Delta 7320 on 15 December 1999.

Overall direction of the EO-1 mission and acquisition of the spacecraft is being carried out by the Goddard Space Flight Center (GSFC) of NASA. MIT Lincoln Laboratory developed the Advanced Land Imager with NMP Instrument Technology and Architecture team members Raytheon Systems Santa Barbara Remote Sensing (SBRS) for the focal plane system and SSG Inc. for the optical system. Lincoln Laboratory was responsible for the design, fabrication, test and development of the instrument, the software and databases for calibration, and will be responsible for the initial on-orbit performance assessment. The mechanical and electronic design features are described in detail by Bicknell et al.[1] Detailed descriptions of ALI testing, data processing, and performance results are given elsewhere. [2-10] The integration and test effort at MIT Lincoln Laboratory has been completed and the instrument was delivered to NASA in March 1999. The ALI is now installed on the spacecraft

* Correspondence: Tel. 781-981-7996, Fax. 781-981-4608, Email: lencioni@ll.mit.edu

and has been successfully operated with the spacecraft C&DH electronics and data have been recorded and faithfully replayed from the Wideband Advanced Recorder-Processor (WARP).

2. ALI DESIGN AND OPERATION

A conceptual sketch of the ALI illustrating the major design features is shown in Figure 1. The telescope is a f/7.5 reflective triplet design with a 12.5 cm unobscured entrance pupil and a FOV of 15° cross-track by 1.256° in-track. It employs reflecting optics throughout, to cover the fullest possible spectral range. The design uses four mirrors: the primary is an off-axis asphere, the secondary is an ellipsoid, and the tertiary is a concave sphere, and the fourth is a flat folding mirror. This technology will enable the use of large arrays of detectors at the focal plane, for covering an entire 185 km swath equivalent to Landsat in a "push broom" mode. The optical design features a flat focal plane and telecentric performance, which greatly simplifies the placement of the filter and detector array assemblies. The design incorporates silicon carbide mirrors and an Invar truss structure with appropriate mounting and attachment fittings. Silicon carbide has many favorable properties for space optical systems. It possesses a high stiffness to weight ratio, a high thermal conductivity, and a low coefficient of thermal expansion.

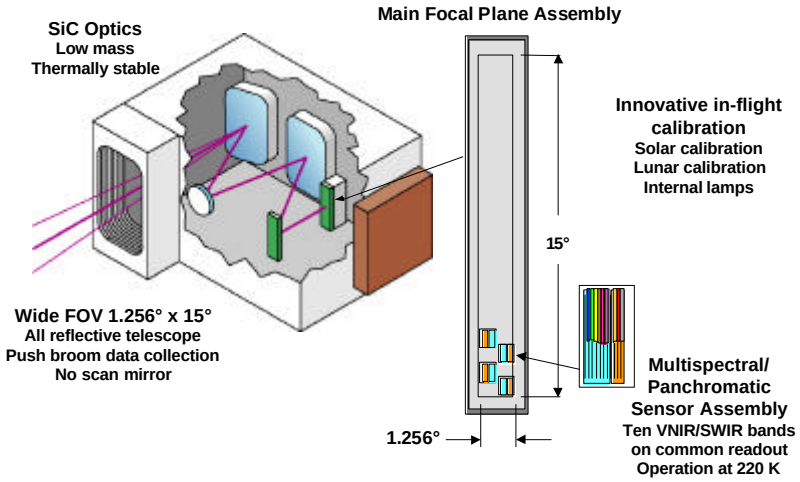

Figure 1. A conceptual sketch of the ALI telescope and Focal Plane Assembly.

Although the optical system supports a 15° wide FOV, only 3° was populated with detector arrays as illustrated in Figure 2. The multispectral panchromatic (MS/Pan) array has 7 spectral bands in the visible and near infrared (VNIR), and 3 in the short wave infrared (SWIR). The Pan detectors subtend 10 m square pixels on the ground and are sampled every 10 m as the earth image moves across the array. The MS detectors subtend 30 m and are sampled every 30 m. The wavelength coverage and ground sampling distance (GSD) are summarized in Table 1. The wavelength intervals were chosen for comparison with Enhanced Thematic Mapper (ETM+) on Landsat 7 and for other science objectives.

Four sensor chip assembles (SCA's) populate the 3° cross-track segment of the focal plane. Each MS band on each SCA contains 320 detectors in the cross-track direction, while each pan band contains 960 detectors. The total cross-track coverage from the single MS/Pan module is 37 km.

The MS/Pan arrays use Silicon-diode VNIR detectors fabricated on the Silicon substrate of a Readout Integrated Circuit (ROIC). The SWIR detectors are Mercury-Cadmium-Telluride (HgCdTe) photo-diodes that are Indium bump-bonded onto the ROIC that services the VNIR detectors. These SWIR detectors promise high performance over the 0.9 to 2.5 μm wavelength region at temperatures that can be reached by passive or thermoelectric cooling. The nominal focal plane temperature is 220K and is maintained by the use of a radiator and heater controls.

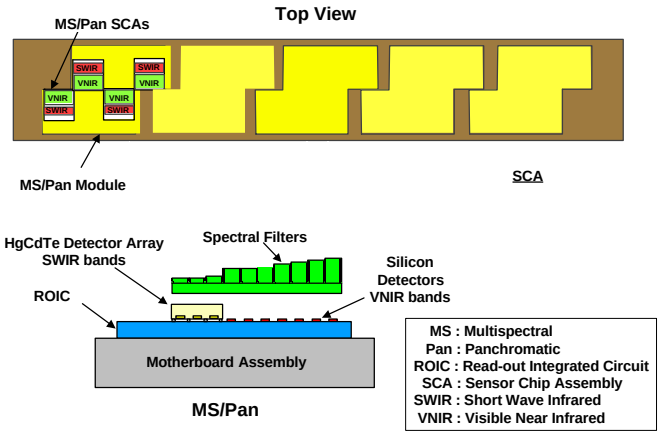

Figure 2. Focal Plane Assembly.

Band	Wavelength (μm)	GSD (m)
Pan	0.480-0.690	10
MS-1’	0.433-0.53	30
MS-1	0.450-0.515	30
MS-2	0.525-0.605	30
MS-3	0.630-0.690	30
MS-4	0.775-0.805	30
MS-4’	0.845-0.890	30
MS-5’	1.200-1.300	30
MS-5	1.550-1.750	30
MS-7	2.080-2.350	30

Table 1. Summary of the ALI Spectral Coverage and Ground Sample Distances

Application of detectors of different materials to a single readout integrated circuit (ROIC) enables a large number of arrays covering a broad spectral range to be placed closely together. This technology is extremely effective when combined with the wide cross-track FOV optical design being used on the ALI.

Both the array frame rate and the detector integration time can be set by commands to the Focal Plane Electronics (FPE). The nominal MS frame rate is 226 frames/sec and for the PAN it is 678 frames/sec. The nominal integration times are 4.05 msec for the MS detectors and 1.35 msec for the Pan. The frame rate can be adjusted in 312.5 nsec increments to synchronize frame rate with ground scan velocity variations due to altitude and velocity variations during orbit. The integration times can also be selected over a range from 0.81 ms to 4.86 ms in steps of 0.27 ms for the MS detectors. The corresponding values for the Pan band are one third of those for the MS bands. The FPE samples the output of each detector with a 12-bit converter. The digitized data are then sent to the solid-state recorder onboard the spacecraft.

A photograph of the integrated flight telescope and FPA but without the external housing is shown in Figure 3.

Telescope features

- **12.5 cm entrance pupil**
- **15° x 1.26° field-of-view**
- **Telecentric, f/7.5 design**
- **Unobscured, reflective optics**
- **Silicon carbide mirrors**
- **Wavefront error = 0.11 λ RMS @ 633 nm**

Figure 3. Flight ALI mounted on the aluminum flight pallet prior to the housing installation. Note the external calibration source mounted on the left side of the metering truss.

The completely assembled ALI can be seen in Figure 4. The approximately 0.9m (X) x 0.9m (Y) x 0.7m (Z) size instrument sits on an aluminum pallet that attaches to the spacecraft. In orbit the instrument is wrapped in Multi-Layer Insulation (MLI). The thermal radiators for the Focal Plane (visible in Figure 4.) and the Focal Plane Electronics are outside the MLI wrap. The telescope is under the MLI surrounded by a thin (~1mm) aluminum housing that supports an aperture cover. The ALI Control Electronics and the Focal Plane Electronics (FPE) packages are supported on the pallet outside the telescope housing.

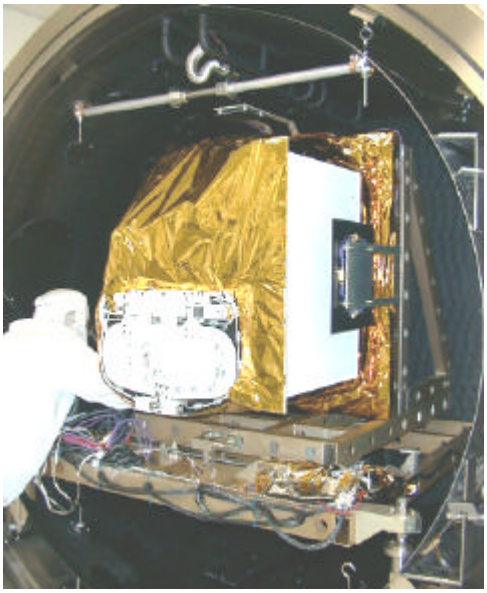

Figure 4. ALI being placed into thermal-vacuum test chamber.

3. ALI CALIBRATION PLAN

The calibration and characterization plan for the ALI has both pre-launch and in-flight components. The objectives are to characterize the overall instrument performance and to determine all instrument parameters required to generate accurate estimates of spatial, spectral and radiometric image quantities. The ALI performance requirements were guided by the Landsat 7 specification [14] and were generated in concert with Landsat, EOS and EO-1 calibration scientists. The requirements were also constrained by the primary NMP mission objective, which is the validation of enabling technologies in flight. The

instrument performance & verification tests also included measurements of noise, repeatability, polarization dependencies, temperature transient response, saturation recovery, image artifacts, and stray light rejection.

3.1 Calibration parameters

The sensor calibration data comprise five measurement categories and are established for each detector channel (N). These are:

a) Normalized spectral response function: $F_N(l)$

This function represents the relative response of a detector channel to a constant monochromatic radiance ($W/cm^2 * sr * \mu m$) at the entrance aperture of the sensor as a function of wavelength. The function is normalized to unity at the peak. These functions define the in-band radiance (L_λ) at the entrance of the sensor:

$L_\lambda = \int L(\lambda)F_N(\lambda)d\lambda$, where $L(\lambda)$ is the spectral radiance at the entrance of the sensor.

a) Pixel angular position in object space: $(x, y)_N$

Each detector will respond to the radiance from different angular directions. This direction is determined both by the location of the detector in the focal plane of the telescope and the distortion from the optical system. Undistorted reconstruction of a ground scene requires accurate knowledge of the relative angular position of each detector in object space. These are measured relative to an arbitrary but known bore-sight direction.

a) Modulation transfer function: MTF_N

The MTF for each detector channel is a two dimensional function of the spatial frequency of the imaged scene. It represents the magnitude of the Fourier transform of the detector channel's system response as a function of angle. The MTF is a measure of image sharpness and is used in quantitative image reconstruction.

a) Zero signal digital number offset: dn_o,

This is the digital number offset that each detector channel has when there is no input radiance. These offsets remain fairly constant, however they are measured for every data collection event to improve accuracy.

a) Response coefficient: C_N,

These convert raw digital numbers (dn) to estimates of in-band radiance (L^*_λ), i.e., $L^*_\lambda = C_N (dn - dn_o)$. Although C_N is approximately constant over the full dynamic range it is in general a weak function of $(dn - dn_o)$. This is accounted for in the calibration process. Each detector channel has 16 functional representations for C_N, one for each integration time.

These five calibration "parameters" are built up from all the pre and post launch measurements. A summary of this process, including the relative weight of each measurement, is shown in Table 2. Note that there is at least one primary measurement for each of the five "parameters" and that only for the spectral response functions are there no on-orbit measurement of significant value.

	Spectral Response Function	Response Coefficient	Zero Signal Offset	Pixel Angular Position	Modulation Transfer Function
Component Tests and Analysis	●	○	—	—	○
Subsystem Tests: Telescope and MS/Pan	—	○	○	○	○
Instrument-Level Laboratory Tests	●	●	○	●	●
On-Orbit Measurements:					
Solar Diffuser	—	●	—	—	—
Closed Aperture	—	—	●	—	—
Internal Source	—	○	—	—	—
Lunar Scans	—	○	○	—	○
Earth Scenes	—	○	—	○	○

Table 2. ALI calibration matrix. Primary measurements are denoted by solid circles and secondary measurements by open circles. A dash indicates that no data of any significant value is obtained.

3.2 Pre-launch calibration and characterization strategy

The pre-launch calibration, which is essentially completed, began with testing and analysis at the component level. This process continued through subsystem and system level testing. The objective was to generate initial estimates of the sensor's spatial, spectral, and radiometric characteristics and then track the performance throughout the development phases of the instrument. This provided an early indication of any test setup errors, analysis errors, or performance anomalies. Moreover, since this process employed a number of independent and complementary calibration methods, consistency in projected performance increased the confidence of the final calibration parameters. Pre-launch testing and calibration were conducted under mission-like conditions including appropriate environmental conditions, and the full range of signal levels, wavelengths and spatial frequencies. The internal calibration source was used throughout ground testing as a health check and to measure stability of performance. This was especially useful during environmental testing as a means of verifying satisfactory performance. Some measure of absolute radiometry is established for the internal calibration source by transfer to the integrating sphere calibration. The design of the internal source is described by Mendenhall et al [6].

3.3 In-flight calibration strategy

The post-launch calibration will begin with internal source measurements. This is the only direct link to the pre-launch calibration and establishes continuity of performance from ground to space. The on-orbit absolute calibration relies primarily on solar calibration. For solar calibration there is motor-driven aperture selector in the aperture cover assembly itself. The aperture selector moves an opaque slide over a row of small to increasingly larger slit openings and then reverses the slide motion to block all light. Just prior to solar calibration, a Spectralon diffuser plate is swung over the secondary mirror by a motor-driven mechanism. The diffuser reflectively scatters the sunlight that would otherwise impinge on the secondary. During solar calibration the reflectively scattered sunlight exposes the FPA to an irradiance that is equivalent to earth-reflected sunlight for an earth albedo ranging from 0 to 100%. This is illustrated in Figure 5. Lunar scans are planned and will be used as a measure of image quality and some (TBD) measure of radiometric accuracy. Finally, well-characterized ground scenes will be used for both image quality assessment and radiometry. The on-orbit calibration plan is intended to contain adequate capabilities for cross checks and diagnostic tests.

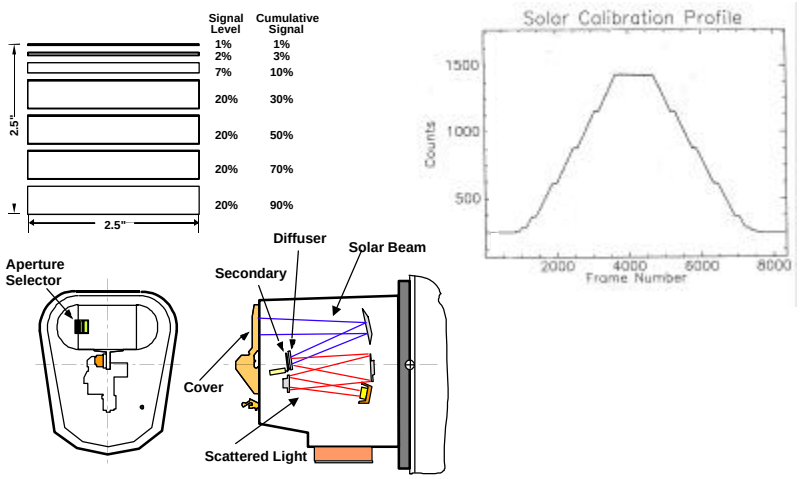

Figure 5. Illustration of the solar calibration mode and detector data from the laboratory functional test using a solar simulator.

4. FACILITIES AND EQUIPMENT

All testing and calibration of the ALI were carried out in a Class 1,000 clean room at Lincoln Laboratory. Most of the major assembly, such as integration of the focal plane with the optical system and some functional measurements requiring only the VNIR detectors, were done under a class 100 laminar flow module located within the clean room. The definitive calibration and characterization measurements on the ALI were performed while the instrument was in the thermal vacuum chamber that contained a liquid nitrogen-cooled shroud (see Figure 4). The SWIR detectors of the ALI required cooling to 220K and could not be tested otherwise. Moreover the entire ALI was operated at flight temperature and vacuum conditions. Three major

optical test configurations were used for most of the key measurements. These consisted of a Schmidt sphere imaging collimator, an off-axis parabolic collimator, and a 30 inch integrating sphere with a spectro-radiometer. [2-7] With the ALI in the vacuum chamber, optical measurements were made through a 12 inch diameter fused-silica window. This window was well characterized for both wavefront error and spectral transmission. A summary of the major ALI performance tests and the corresponding test configurations is given in Table 3. The Landsat transfer calibration was the only test not done in the clean room.

TASK	OPTICAL TEST CONFIGURATION
FPA alignment	Schmidt sphere imaging collimator with knife edge
Focus verifications	Schmidt sphere imaging collimator with knife edge
End-to-end imaging	Schmidt sphere imaging collimator with scene
MTF measurements	Schmidt sphere imaging collimator with knife edge
Pixel line-of-sight	Schmidt sphere imaging collimator with Ronchi ruling
Image of filters	Schmidt sphere imaging collimator with CCD camera
Reference cube alignment	Autocollimating theodolite
Spectral calibration	Off-axis parabolic collimator and grating monochromator
Polarization tests	Off-axis parabolic collimator with Glan-Thompson prisms
Solar calibration functional test	Off-axis parabolic collimator with a 1kW Xe arc lamp and a Spectralon diffuser
Radiometric calibration	Integrating sphere and spectroradiometer
Landsat transfer calibration	Integrating sphere and GSFC LXR
Internal source transfer calibration	Internal source

Table 3. Summary of the major ALI performance tests and the corresponding test configurations.

5. PRELIMINARY RESULTS

The ALI performance and calibration data that were collected are still in the process of being analyzed. Detailed results to date are reported by Hearn et al, [4] Mendenhall et al, [5,6] Evans et al, [12] and Viggh et al. [11,13] This section provides some representative data which illustrate the overall performance of the ALI.

The internal calibration source provides three illumination levels plus a zero signal reference. It is mounted on the side of the telescope metering truss and illuminates the FPA from an angle of about 30^0 relative to the normal. This produces a gradient in the illumination and a shadowing near the edges of the four SCA's caused by the filter bezels. An example of the detector outputs for the three lamp levels is shown in Figure 6. The zero signal offsets have been subtracted from these data. This particular example shows the signals for all 1240 detectors in MS Band # 4. A very useful and sensitive diagnostic technique for determining the stability of the ALI consisted of monitoring the outputs of the detectors during a series of tests or over a period of time. The ratio of outputs for each detector from Band # 4 measured 5 days apart is shown in Figure 7.

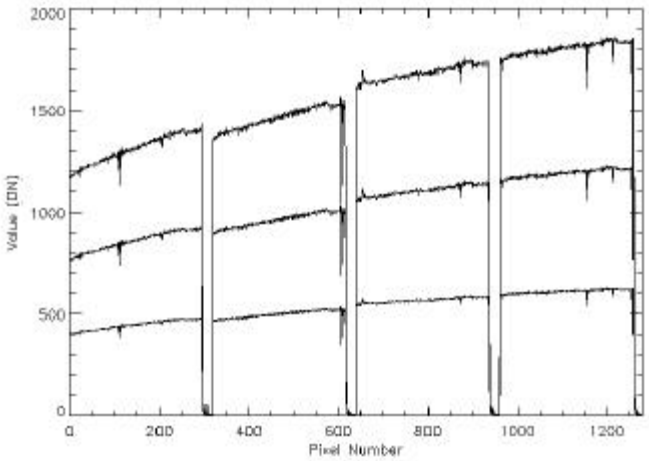

Figure 6. Band # 4 detector outputs for the three internal calibration lamp levels.

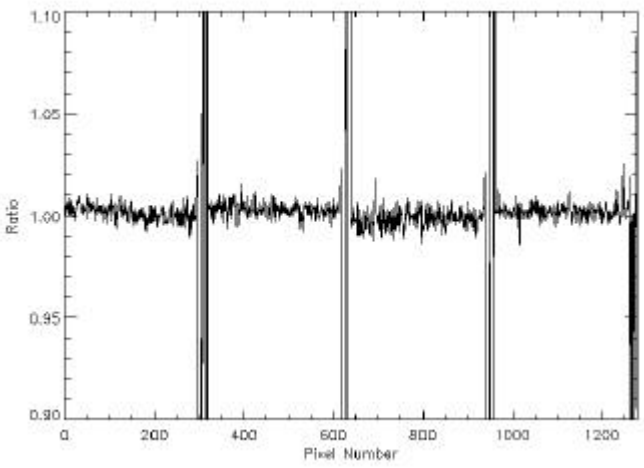

Figure 7. The ratio of outputs for each detector from Band # 4 measured 5 days apart.

There were two primary methods used to determine the normalized spectral response functions in our calibration plan. The first relies on combining the individual component measurements, i.e., the spectral reflectance of the four mirrors, the transmissions of the filters, and the detector responses. The product of these terms when normalized to the peak is expected to give an accurate estimate of the system response. Note that errors in this function are of second order since the magnitude of the transmission is carried in the response coefficients C_N . Nevertheless measurements were also made at the system level to to detect effects such as vacuum induced changes, contamination, etc. The two approaches have thus far been compared only in the VNIR bands and have indicated excellent agreement. An example is given in Figure 8 for Band 3.

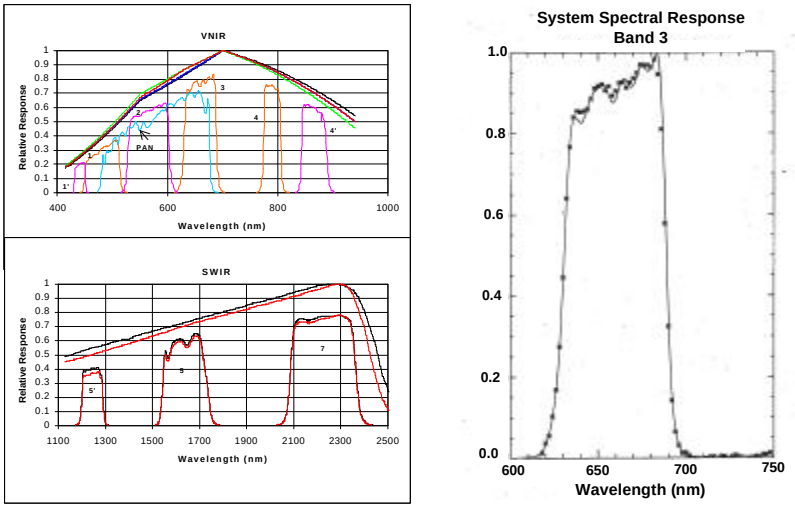

Figure 8. Spectral response functions obtained form component measurements are shown on the left. The normalized spectral response function for a sensor level measurement is compared to the calculated value from component measurements on the right.

The integration of the ALI focal plane system with the telescope required determining the proper thickness for the shim which would place the FPA at the best-focus plane of the telescope. This was accomplished with the imaging collimator [2,7] by making successive knife-edge scans, with the plane of the knife-edge displaced by various distances from the true collimator focus position. For each scan, a figure-of-merit, such as the full width at half maximum of the detector line spread function normalized to the detector width,. was calculated, indicating the relative quality of the focus The figures of merit were plotted, and the position of the knife-edge was found which gave the best focus. The distance of that position from the true collimator focus, when multiplied by the square of the ratio of focal lengths (ALI telescope to collimator), was the estimated focus error in the ALI. The FPA was then removed, the shim was corrected, and the process was repeated. In this case, only one cycle of shim adjustment was made. This process is depicted in Figure 9.

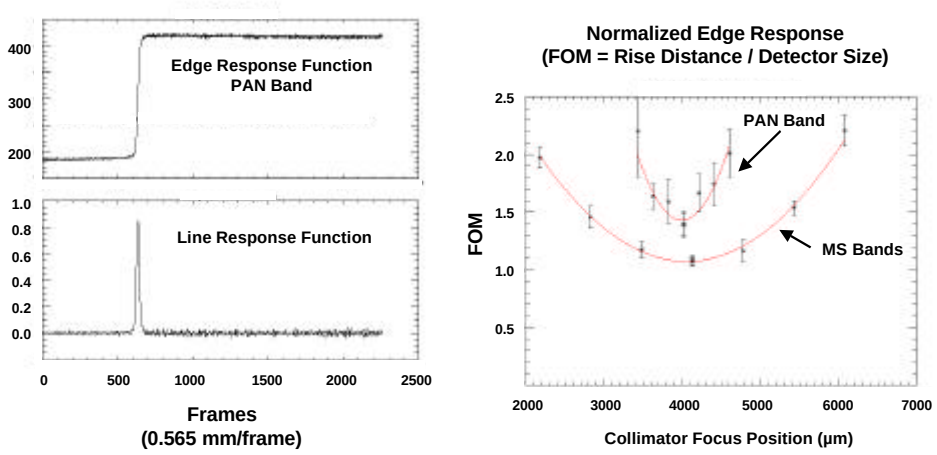

Figure 9. Focus test data used to find the correct shim thickness for integrating the telescope and focal plane array.

To measure the system MTF's of the ALI, knife-edge scans were made across representative pixels of each band and each sensor chip assembly (SCA), in both cross-track and in-track directions. These were generated by scanning the knife edge at the focus of the imaging collimator and projecting the beam into the ALI which was in the thermal vacuum chamber. The detected signals, when normalized to a response range of zero (black) to one (white), represent the edge-spread function (ESF) of each pixel. The derivative of the ESF is the line-spread function (LSF). The Fourier transform of the detector channel's LSF provides the MTF's. An example of this process is given in Figure 10. More detail is given by Hearn et al. [2]

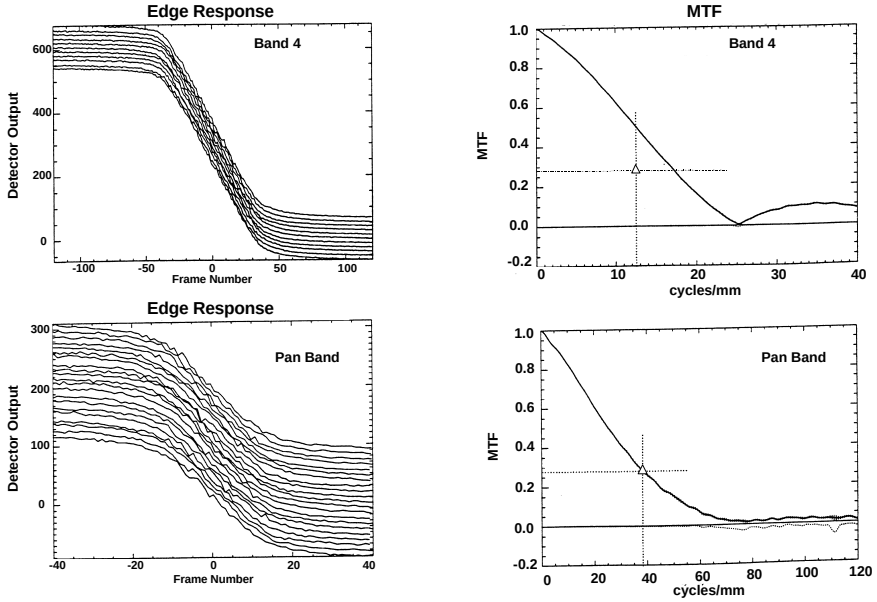

Figure 10. Edge response functions and the corresponding MTF's for MS Band 4 and the Pan Band.

The overall imaging performance was verified by end-to-end imaging tests in which collimated target images, scanned at the earth rate that will be seen on-orbit, were injected into the ALI. The reconstructed and calibrated image of a Star Burst target for the Pan Band is shown in Figure 11. For this case the image was generated with all four SCA's. At the inner circle of the Star Burst the lines are about 1.8 pixels wide (equivalent to 18 m on the ground) and can easily be resolved in the expanded view.

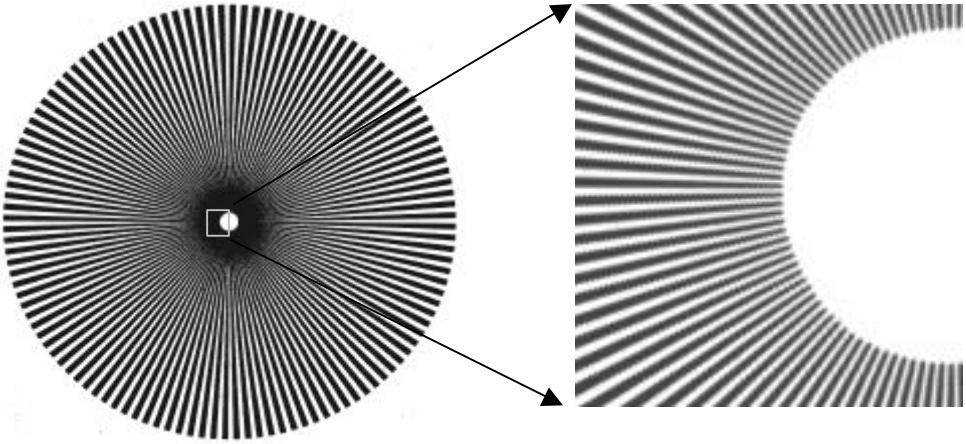

Figure 11. End-to- end reconstruction of a Star Burst image in the Pan Band

The ALI is designed to operate with out saturating over the full range from 0% to 100% albedo with 12 bit resolution. The instrument was calibrated over this full range. An example of the output of one detector over its full dynamic range is given in Figure 12. For this example the input was varied by changing both the radiance and the ALI integration times. The full dynamic range defined as the ratio of the saturation flux to the RMS noise is in this case 3.8×10^3.

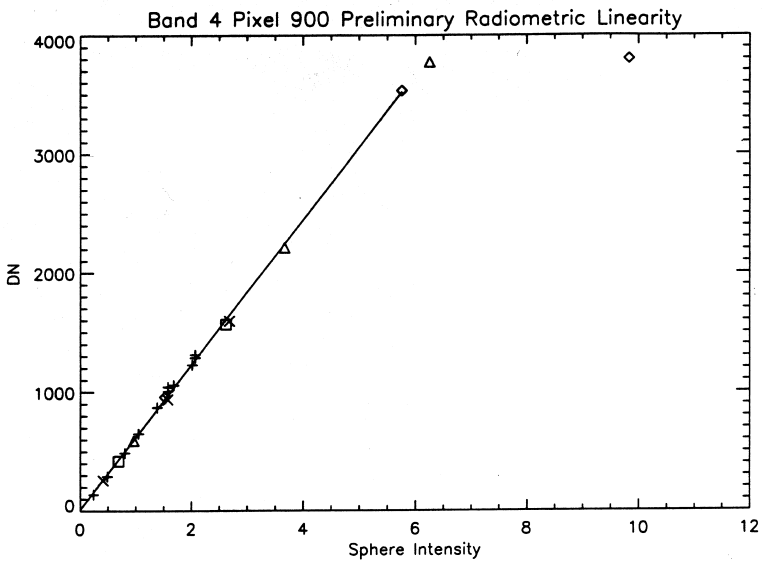

Figure 12. ALI dynamic range and linearity for a typical pixel (# 900, Band # 4)

One of the most significant performance aspects of the ALI is the high SNR that is achieved with such a small optical aperture (12.5 cm). This is illustrated in Figure 13. which summarizes the average SNR of all the bands for a 5% earth surface reflectance. These results are compared to the SNR of the ETM+. In the bands that are common to both instruments, the expected ALI SNR ranges from 4 to 10 times greater than ETM+. This enhanced SNR is the result of the large number of detectors and the increase in integration time inherent in the push broom architecture.

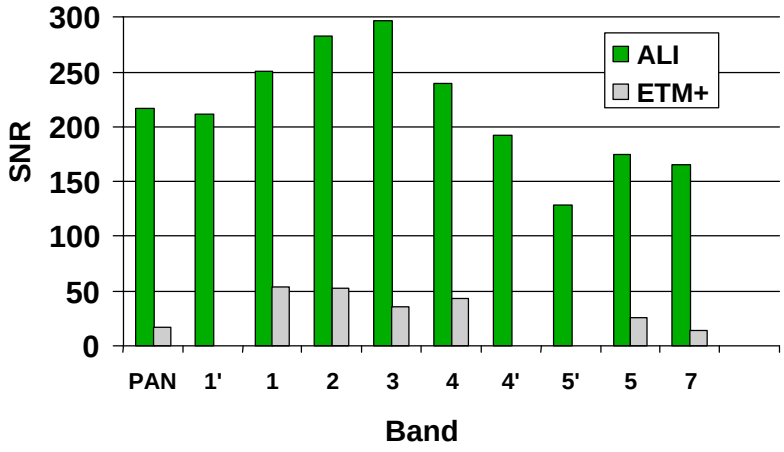

Figure 13. ALI and ETM+ SNR performance for a 5% earth surface reflectance

7. APPLICATION TO FUTURE LANDSAT INSTRUMENT

One key element of the NMP technology validation for the ALI is the demonstration of scalability to a full up Landsat instrument. Several design features and tests have accomplished this result. The FPA was designed in a modular fashion so that the full 15^0 coverage could be achieved by simply replicating the ALI module four more times. The data rate increases by a factor of 5 while it is estimated that the electrical power of the FPA would increase about a factor of 3. There would be no physical changes in the instrument design to accommodate this upgrade. Moreover, the optical subsystem performance was verified over the full 15^0 field of view. The placement of the populated detector module on the outer 3^0 of the available field was done deliberately to validate the most stressing portion of the FOV. An ALI with an fuly populated FPA would exhibit about one-fourth the mass, one-fifth the power, and about one-third the volume compared to the ETM+ of Landsat 7. These along with the improved SNR make the EO-1 ALI design and technologies very attractive for use in future missions.

SUMMARY

The EO-1 Advanced Land Imager has undergone extensive pre-launch characterization and calibration. Although data analysis and performance assessments are still in progress, preliminary results indicate superior performance in resolution, image quality, SNR, dynamic range, radiometric accuracy, and repeatability. This performance has been achieved in a sensor of considerably smaller size, lower weight, and requiring less power then previous instruments with similar Earth observing objectives. The EO-1 mission should successfully flight-validate the New Millennium Program technology and science objectives. It also provides a path for a lower cost, higher performance, Landsat follow-on.

ACKNOWLEDGEMENTS

This work was sponsored by NASA/Goddard Space Flight Center under U.S. Air Force Contract number F19628-95-C-0002. Opinions, interpretations, conclusions, and recommendations are those of the authors and are not necessarily endorsed by the United States Air Force. The authors want to acknowledge the programmatic support and technical contributions from William M. Brown, Jr, Dr. Charles Bruce, and Dr. Steven Forman of MIT Lincoln Laboratory.

REFERENCES

1. W.E. Bicknell, C. J. Digenis, S. E. Forman, D. E. Lencioni, “EO-1 Advanced Land Imager”, *SPIE Conference on Earth Observing Systems IV*, Denver, Colorado, 18 July 1999.
2. D. R. Hearn, J. A. Mendenhall, B. C. Willard, "Spatial calibration of the EO-1 Advanced Land Imager," *SPIE Conference on Earth Observing Systems IV*, Denver, Colorado, 18 July 1999.
3. J. A. Mendenhall, A. C. Parker, "Spectral calibration of the EO-1 Advanced Land Imager, "*SPIE Conference on Earth Observing Systems IV*, Denver, Colorado, 18 July 1999.
4. J. A. Mendenhall, D. E. Lencioni, A. C. Parker, "Radiometric calibration of the EO-1 Advanced Land Imager," *SPIE Conference on Earth Observing Systems IV*, Denver, Colorado, 18 July 1999.
5. J. A. Mendenhall, D. E. Lencioni, D. R. Hearn, and A. C. Parker, “EO-1 Advanced Land Imager preflight calibration,” Proc. SPIE, Vol. 3439, pp.390-399, July 1998.
6. J. A. Mendenhall, D. E. Lencioni, D. R. Hearn, and A. C. Parker, “EO-1 Advanced Land Imager in-flight calibration,” Proc. SPIE, Vol. 3439, pp.416-422, July 1998.
7. B. C. Willard, “Wide field-of-view Schmidt-sphere imaging collimator,” *SPIE Conference on Earth Observing Systems IV*, Denver, Colorado, 18 July 1999.
8. H. Viggh, J. Mendenhall, R. Sayer, J. S. Stuart, M. Gibbs, "An Automated Ground Data Acquisition and Processing System for Calibration and Performance Assessment of the EO-1 Advanced Land Imager", *SPIE Conference on Earth Observing Systems IV*, Denver, Colorado, 18 July 1999.
9. J. Evans, H. Viggh, "Radiometric Calibration Pipeline for the EO-1 Advanced Land Imager", *SPIE Conference on Earth Observing Systems IV*, Denver, Colorado, 18 July 1999.
10. H. Viggh, J. S. Stuart, R. Sayer, J. Evans, M. Gibbs, "Performance Assessment Software for the EO-1 Advanced Land Imager", *SPIE Conference on Earth Observing Systems IV*, Denver, Colorado, 18 July 1999.
11. “Landsat 7 System Specification”, Revision K, NASA Goddard Space Flight Center, 430-L-0002-K, July 1997